Charge exchange reactions as tests for structures of exotic nuclei

S. Karataglidis and I. A. Wright
Department of Physics and Electronics, Rhodes University, P. O. Box 94, Grahamstown, 6140, South Africa

Abstract
Charge exchange reactions serve as alternative tests of the structures of exotic nuclei. Of particular relevance is the (p,n) reaction, which is related to the Gamow-Teller matrix element. The (p,n) reaction is also related to (p,p') in the case of transitions to the isobaric analogue state (IAS). There are few measurements of (p,n) reactions using exotic beams. We revisit the case of ^{6}He$(p,n)^6$Li and discuss apparent discrepancies with other available data.

1 Introduction

Charge exchange reactions are an important alternative to scattering as sensitive tests of nuclear structure. In the case of photon-induced reactions, $(\gamma\pi^{\pm})$ reactions on stable nuclei may lead to exotic nuclear states, including the population of excited states, as was illustrated in the case of ^{17}O$(\gamma,\pi^-)^{17}$F [1], and of ^{6}Li$(\gamma,\pi^+)^6$He [2]. The latter was recently measured at the tagged photon facility at Mainz MAMI-B [3], to resolve discrepancies associated with earlier measurements using bremsstrahlung.

The simplest hadron-induced charge exchange reactions are (p,n) and (n,p). These are of interest as: (a) the exchange reaction proceeds primarily through the isovector part of the nucleon-nucleus (NA) optical potential; (b) the matrix elements of the transition relate to the Gamow-Teller (GT) matrix elements; and (c) the (p,n) reaction is related to (p,p') scattering in the case of transitions involving isobaric analogue states. The relationship to the GT transitions is important as ground state halos are particle-bound but β-decay through the GT matrix element. Hence (p,n) reactions are investigated in radioactive beam experiments using hydrogen targets. One such case, which we consider herein, is the ^{6}He$(p,n)^6$Li reaction to the ground and isobaric analogue states in ^{6}Li, which was measured at GANIL by the Saclay group [4]. Those data, which used a $41.6A$ MeV ^{6}He beam incident on a hydrogen target, were analysed using the JLM optical model, but the analysis required a very large increase in the strength of the imaginary potential ($\lambda_W = 1.8$) in order to explain the very small differential cross sections measured.

This paper will present a reanalysis of those data, using the Melbourne g-folding optical model [5], and discuss the connection to the available ^{6}He(p,p) and ^{6}He(p,p') data taken at the same energy [6].

2 Charge exchange reactions in the Melbourne optical model

The Melbourne optical model, or Melbourne g-folding model, is extensively described in the review article [5], to which we refer the reader. We present the salient points herein as they relate to the description of charge exchange reactions.

The basis for the optical potential are the g matrices, which are the momentum-space solutions of the Brueckner-Bethe-Goldstone (BBG) equation in infinite matter, *viz*

$$g^{(JST)}_{LL'}\left(p\,p;k,k_f\right) = V^{(JST)}_{LL'}\left(p,p'\right) + \frac{2}{\pi}\sum_l \int_0^\infty V^{(JST)}_{Ll}\left(p',q\right)\left[\mathcal{H}\right] g^{(JST)}_{lL'}\left(q,p;k,k_f\right)\, q^2 dq, \quad (1)$$

where

$$\mathcal{H} = \frac{\bar{Q}(q,K;k_f)}{\bar{E}(q,K;k_f) - \bar{E}(k,K;k_f)}, \quad (2)$$

in which $\bar{Q}(q,K;k_f)$ is an angle-averaged Pauli operator with an average centre-of-mass momentum K, and the energies $\bar{E}$ are medium-modified by the use of auxiliary potentials using the prescription

of Haftel and Tabakin [7]. The $V_{LL'}^{JST}$ is the nucleon-nucleon (NN) interaction. Those g matrices are dependent on the (two-body) total angular momentum, J, spin, S, and isospin, T. In that respect, one obtains the isoscalar and isovector optical potentials self-consistently from the same set of g matrices.

The effective NN interaction, which contain central, tensor, and two-body spin-orbit terms, is then obtained in ST channel form by mapping onto coordinate-space representations as sums of Yukawa potentials, *viz.*

$$g_{\text{eff}}^{ST}(r,\omega) = \sum_i \langle\theta_i\rangle \sum_{j=1}^{n_i} S_j^{(i)}(\omega)\frac{e^{-\mu_j^{(i)}r}}{r}, \tag{3}$$

where the θ_i are the characteristic operators for central forces ($i = 1$), containing $\{1, (\sigma\cdot\sigma), (\tau\cdot\tau), (\sigma\cdot\sigma\tau\cdot\tau)\}$ terms, for the tensor force ($i = 2$), and for the two-body spin-orbit force ($i = 3$). The $S_j^{(i)}(\omega)$ are complex, energy- and medium-dependent strengths, and $\mu_j^{(i)}$ are the inverse ranges of the interaction. The number of strengths and inverse ranges n_i can be as large as necessary; $n_i = 4$ is sufficient to reproduce the on-shell and a range of half-off-shell g matrices within 32 NN S,T channels.

From the g matrices, as mapped onto coordinate space representations, the optical potential for elastic scattering may be written as

$$U(\mathbf{r}_1,\mathbf{r}_2) = \delta(\mathbf{r}_1-\mathbf{r}_2)\sum_n \zeta_n \int \varphi_n^*(\mathbf{s}) v_{\text{D}}(R_{1s})\varphi_n(\mathbf{s})\, d\mathbf{s} + \sum_n \zeta_n \varphi_n^*(\mathbf{r}_1) v_{\text{Ex}}(R_{12})\varphi_n(\mathbf{r}_2), \tag{4}$$

where $R_{ij} = |\mathbf{r}_i - \mathbf{r}_j|$. The summation is over the shells defined in the basis from the nuclear structure model used in the calculation of the density, with ζ_n being the occupation numbers for each shell as obtained from the one-body density matrix elements (OBDME). The subscripts D and Ex denote the sets of elements of the effective interaction defining the direct and exchange parts of the NA optical potential, respectively. Those interactions, v_{D} and v_{Ex}, are complex and energy dependent by construction as the effective interaction is derived from the g matrices defined above. Note that the direct part of the optical potential is the familiar $g\rho$ form of the optical potential, *viz.*

$$\begin{aligned} V_{\text{D}}(\mathbf{r}_1) &= \delta(\mathbf{r}_1-\mathbf{r}_2)\sum_n \zeta_n \int \varphi_n^*(\mathbf{s}) v_{\text{D}}(R_{1s})\varphi_n(\mathbf{s})\, d\mathbf{s} \\ &= \delta(\mathbf{r}_1-\mathbf{r}_2)\int \rho(\mathbf{s}) v_{\text{D}}(R_{1s})\, d\mathbf{s}. \end{aligned} \tag{5}$$

The nonlocality in the optical potential comes explicitly from the exchange term in Eq. (4). Neglect of that term leads to serious problems in the descriptions of scattering processes [8].

Inelastic scattering and charge exchange reactions may be described in the distorted wave approximation (DWA), with the effective NN interaction defining the optical potential taken as the transition operator. The transition amplitude is, with '0' denoting the projectile and '1' denoting the bound nucleon in the nucleus,

$$\begin{aligned} T &= T_{J_f J_i}^{M_f M_i \nu\nu'}(\theta) \\ &= \left\langle \chi_{\nu'}^{(-)}(\mathbf{k}_{\text{o}}0)\right| \left\langle \Psi_{J_f M_f}(1\ldots A)\right| A g_{\text{eff}}(0,1)\mathcal{A}_{01} \left\{ \left|\chi_{\nu}^{(+)}(\mathbf{k}_{\text{i}}0)\right\rangle \left|\Psi_{J_i M_i}(1\ldots A)\right\rangle \right\}, \end{aligned} \tag{6}$$

where the distorted wave functions are denoted by $\chi_\nu^\pm$ for an incoming/outgoing nucleon with spin projection ν, wave vector $\mathbf{k}$, and coordinate set 'q'. $\mathcal{A}_{01}$ is an antisymmetrization operator between the projectile and bound state nucleon. A cofactor expansion of the nuclear state $\Psi_{JM}(1\ldots A)$ is made, with the assumption that all pairwise interactions between the projectile and target nucleons are taken to be the same, *viz.*

$$\left|\Psi_{JM}(1\ldots A)\right\rangle = \frac{1}{\sqrt{A}}\sum_{\alpha m} \left|\varphi_{\alpha m}(1)\right\rangle a_{\alpha m} \left|\Psi_{JM}(1\ldots A)\right\rangle, \tag{7}$$

where $\alpha = \{n, (l, s), j, \tau_z\}$ denotes the set of quantum numbers, exclusive of m, necessary to specify the single-particle state. This allows the transition amplitude to be expanded to form

$$T = \sum_{\alpha_1 m_1 \alpha_2 m_2} \left\langle \Psi_{J_f M_f}(1 \ldots A) \left| a^\dagger_{\alpha_2 m_2} a_{\alpha_1 m_1} \right| \Psi_{J_i M_i}(1 \ldots A) \right\rangle \times \left\langle \chi^{(-)}_{\nu'}(\mathbf{k}_\mathrm{o} 0) \right| \langle \varphi_{\alpha_2 m_2}(1) | \, g_{\mathrm{eff}}(0,1) \mathcal{A}_{01} \left\{ \left| \chi^{(+)}_{\nu}(\mathbf{k}_\mathrm{i} 0) \right\rangle | \varphi_{\alpha_1 m_1}(1) \rangle \right\}, \quad (8)$$

where the nuclear matrix elements are given by (with $\tilde{a}_{\alpha m} = (-1)^{j-m} a_{j-m}$)

$$\begin{aligned} \rho &= \left\langle \Psi_{J_f M_f}(1 \ldots A) \left| a^\dagger_{\alpha_2 m_2} a_{\alpha_1 m_1} \right| \Psi_{J_i M_i}(1 \ldots A) \right\rangle \\ &= \sum_{IN} (-1)^{j_1 - m_1} \langle j_2 \, m_2 \, j_1 \, -m_1 | \, I \, N \rangle \left\langle \Psi_{J_f M_f} \left| \left[a^\dagger_{\alpha_2} \times \tilde{a}_{\alpha_1} \right]^{IN} \right| \Psi_{J_i M_i} \right\rangle \\ &= \sum_{IN} (-1)^{j_1 - m_1} \langle j_2 \, m_2 \, j_1 \, -m_1 | \, I \, N \rangle \frac{1}{\sqrt{2J_f + 1}} \langle J_i \, M_i \, I \, N | \, J_f \, M_f \rangle \, S^{J_i J_f}_{j_1 j_2 I} \end{aligned} \quad (9)$$

with application of the Wigner-Eckart theorem. The OBDME are the reduced matrix elements

$$S^{J_i J_f}_{\alpha_1 \alpha_2 I} = \left\langle \Psi_{J_f} \left\| \left[a^\dagger_{\alpha_2} \times \tilde{a}_{\alpha_1} \right]^{I} \right\| \Psi_{J_i} \right\rangle. \quad (10)$$

The transition amplitude is then expressed, in terms of sums over the OBDME, as

$$T = \sum_{\alpha_1 m_1 \alpha_2 m_2} \sum_{IN} (-1)^{j_1 - m_1} \frac{1}{\sqrt{2J_f + 1}} \langle J_i \, M_i \, I \, N | \, J_f \, M_f \rangle \langle j_2 \, m_2 \, j_1 \, -m_1 | \, I \, N \rangle \, S^{J_i J_f}_{\alpha_1 \alpha_2 I} \times \left\langle \chi^{(-)}_{\nu'}(\mathbf{k}_\mathrm{o} 0) \right| \langle \varphi_{\alpha_2 m_2}(1) | \, g_{\mathrm{eff}}(0,1) \mathcal{A}_{01} \left\{ \left| \chi^{(+)}_{\nu}(\mathbf{k}_\mathrm{i} 0) \right\rangle | \varphi_{\alpha_1 m_1}(1) \rangle \right\}. \quad (11)$$

The choice of single particle wave function is also important in the descriptions of scattering and charge exchange reactions involving exotic nuclei. Following Ref. [6], we choose two sets of single particle wave function. The first is the standard set of harmonic oscillators, with the oscillator parameter set by the requirements of the shell model interaction (in this case). That model we denote "non-halo", as the prescription gives rise for a standard neutron skin in the case of neutron-rich nuclei. To obtain a halo or, more correctly, a more extensive neutron density than the standard skin, we use Woods-Saxon (WS) functions, with the binding energies of the orbits which the valence nucleons occupy set to the single neutron separation energy of the exotic nucleus. Comparison of the two models with data then allows for a proper test of the structure of the exotic nucleus under study. For example, such an approach allowed for an unambiguous identification of the halo in ^{6}He [6].

Once all the pieces have been prescribed, we use the DWBA set of programs of Raynal [9] to obtain the microscopic optical potential and the observables (differential cross section, reaction cross section, analysing power) therefrom.

For the evaluation of the ^{6}He(p, n) reaction, we use the Bonn-B potential [10] as the starting potential in the calculation of the g matrices. The ^{6}He wave functions are those as used in the analyses of the (p, p) and (p, p') data [6], which were obtained from a complete $(0 + 2 + 4)\hbar\omega$ shell model using the Zheng G matrix shell model interactions [11]. (These older interactions are used in preference to the more recent Navrátil set as there have been some concerns associated with those [12].) The oscillator parameter as required for that shell model was set to $b = 1.7$ fm. To specify the ^{6}He halo we use the same set of WS single particle energies as was used in the analyses of the proton elastic and inelastic scattering data [6].

3 Charge exchange reactions involving the IAS

Charge exchange reactions involving transitions to isobaric analogue states (IAS) in the spectrum of the target nucleus. In those instances, inelastic proton scattering and (p, n) reactions are related. Assuming that the IAS has the same underlying wave function, when treating isospin as a good quantum number, the transition amplitudes [Eq. (11)] only differ in the particle isospin Clebsch-Gordon coefficient selecting an outgoing proton or neutron. The differential cross section for the (p, n) reaction then scales against the (p, p') to the IAS in the target spectrum, as measured at the same incident proton energy, as the square of the ratio of those Clebsch-Gordon coefficients. Note that this is an aspect of the nuclear structure of the reaction.

An example is that of ^{12}C$(p, n)^{12}$N$_{\rm gs}$ [13, 14]. The ^{12}N ground state is the isobaric analogue of the 15.11 MeV $1^+; 1$ state in ^{12}C. The (p, n) reaction scales as that to the (p, p') as the ratio,

$$R = \left| \frac{\left\langle \frac{1}{2} \ -\frac{1}{2} \ \frac{1}{2} \ -\frac{1}{2} \middle| 1 \ -1 \right\rangle}{\left\langle \frac{1}{2} \ -\frac{1}{2} \ \frac{1}{2} \ \frac{1}{2} \middle| 1 \ 0 \right\rangle} \right|^2 = 2. \tag{12}$$

The data for both the (p, n) and (p, p') in this case illustrate this factor of two, which is also the case in the calculations of both using the Melbourne g-folding model [14].

4 ^{6}He(p, n) and ^{6}He(p, p')

The reactions involving ^{6}He are special cases. The ground state of ^{6}He is $0^+; 1$ and is the isobaric analogue state of the 3.56 MeV $0^+; 1$ state in ^{6}Li. The ^{6}He(p, n) differential cross section then scales to the elastic scattering cross section with the ratio

$$R = \left| \frac{\left\langle \frac{1}{2} \ -\frac{1}{2} \ \frac{1}{2} \ \frac{1}{2} \middle| 1 \ 0 \right\rangle}{\left\langle \frac{1}{2} \ \frac{1}{2} \ \frac{1}{2} \ \frac{1}{2} \middle| 1 \ 1 \right\rangle} \right|^2 = \frac{1}{2}. \tag{13}$$

The ^{6}He(p, n) differential cross section was measured at an energy of $41.6A$ MeV [4], while the elastic scattering cross section was measured at an energy of $40.9A$ MeV [6], making comparison of the two measured cross sections ideal. The (p, n) cross sections to the ground and IAS in ^{6}Li are shown in Fig. 1. Therein, the differential cross-section data for the ^{6}He(p, n) reaction to the ground and IAS in ^{6}Li, taken at $41A$ MeV, are denoted by the squares and crosses, respectively, while the data for the elastic scattering, taken at 40.9MeV are denoted by the circles. The results for the differential cross sections of calculations made using the Melbourne g-folding model for the ^{6}He(p, n) to the IAS and ground states in ^{6}Li are displayed by the solid and dot-dashed lines, respectively. The dashed line corresponds to the differential cross section to the IAS multiplied by 2.

It is apparent by comparison of the two sets of data [(p, n) and (p, p)] that the differential cross section for elastic scattering is greater than the (p, n) to the IAS by a factor of 30. The result of the calculation of the differential cross section for the (p, n) is greater than the corresponding set of data by a factor of 20. Yet, multiplying that result by a factor of 2 gives the dashed curve in Fig. 1 which agrees reasonably with the data for elastic scattering. Note that, while the magnitudes agree quite well, the momentum transfer dependence is different as the elastic scattering contains contributions from the isoscalar and isovector parts of the optical potential, while the (p, n) reaction is isovector only. But the factor of 1/2, as indicated by Eq. (13), is confirmed between our calculations and the elastic scattering data. It is also noteworthy that the JLM potential used in [4] is not capable of explaining the elastic scattering data as the imaginary strength of that potential is too large. A reanalysis of the elastic scattering using a different weighting of the imaginary potential may be needed. Such analysis may yield a value of λ_W much closer to unity.

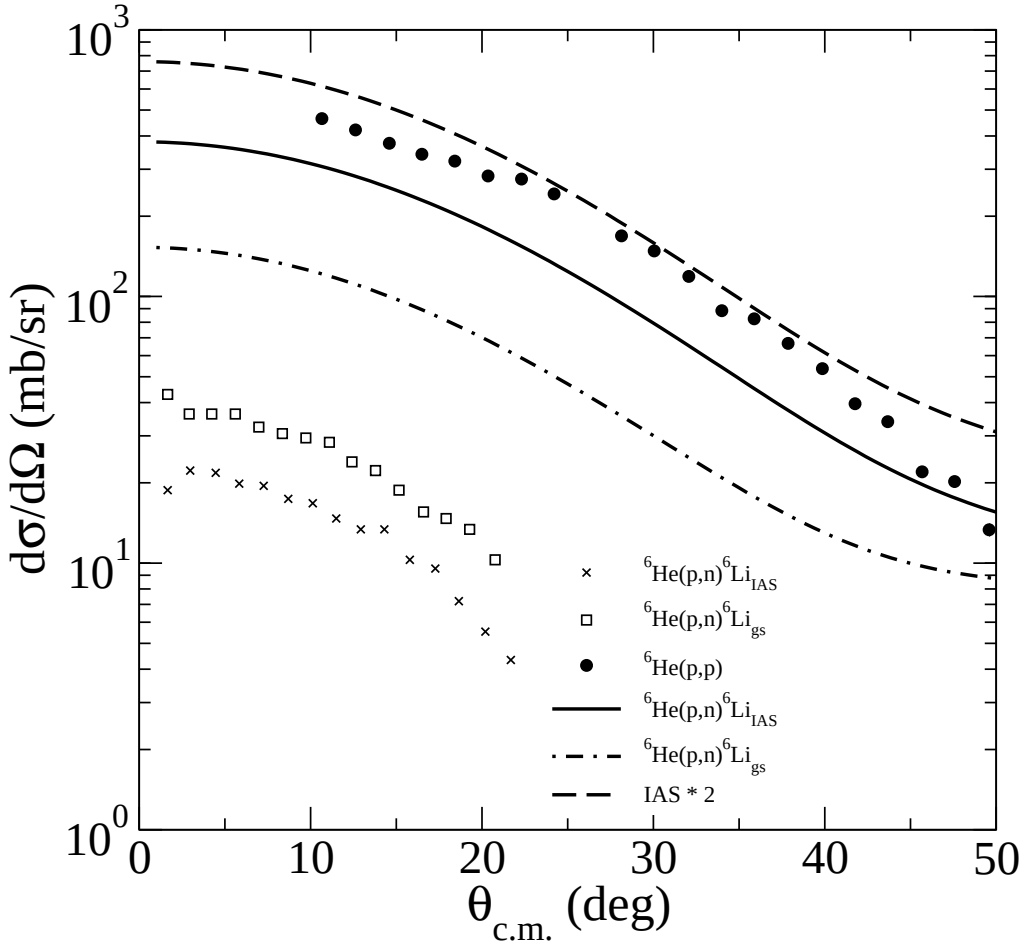

Fig. 1: Differential cross sections for the ^{6}He(p,n) and ^{6}He(p,p) reactions. The data for the (p,n) at $41.6A$ MeV, displayed as squares (ground state transition) and crosses (IAS transition), are taken from Ref. [4], while those of elastic scattering at $40.9A$ MeV, displayed as circles, are taken from Ref. [6]. The results for the (p,n) to the ground and IAS as calculated from the Melbourne g-folding model are the dot-dashed and solid lines respectively. The dashed line is the result of the calculation of the differential cross section to the IAS multiplied by 2.

5 Conclusions

We have presented a new analysis of the available ^{6}He(p,n) reaction data. The results of our calculations of the differential cross sections to both the IAS and ground states in ^{6}Li seriously overestimate the quoted data, but for the IAS the result is in the correct ratio with the available elastic scattering data.

The comparison of the data sets for the elastic scattering and the (p,n) to the IAS is most problematic. Irrespective of the results of our calculations, the data sets do not reflect the ratio of 2 as required by the particle isospin Clebsch-Gordon coefficients, stemming from the nuclear structure, indicating a problem in either of the two measurements. The elastic scattering was a direct measurement of the absolute cross section, while the measurement of the (p,n) was not. Instead it was a relative measurement with the absolute cross section obtained by comparison with available ^{6}Li$(n,p)^6$He data. It would seem that a problem may then lay in the analyses of the (p,n) data, although only a new measurement of that reaction can only confirm it. It is hoped that such a measurement is done with a measurement also of the elastic scattering to ensure that the optical potentials used in the analyses are properly defined.

References

[1] S. Karataglidis and C. Bennhold, Phys. Rev. Lett. **80**, 1614 (1998).

[2] S. Karataglidis, P. J. Dortmans, K. Amos, and C. Bennhold, Phys. Rev. C **61**, 024319 (2000).

[3] N. P. Harrington, *et al.*, Phys. Rev. C **75**, 044311 (2007).

[4] M. D. Cortina-Gil, *et al.*, Nucl. Phys. **A641**, 263 (1998).

[5] K. Amos, P. J. Dortmans, H. V. von Geramb, S. Karataglidis, and J. Raynal, Adv. Nucl. Phys. **25**, 275 (2000).

[6] A. Lagoyannis, *et al.*, Phys. Lett. **B518**, 27 (2001).

[7] M. I. Haftel and F. Tabakin, Nucl. Phys. **A158**, 1 (1970).

[8] P. Fraser, K. Amos, S. Karataglidis, L. Canton, G. Pisent, and J. P. Svenne, Eur. Phys. J. A **35**, 69 (2008).

[9] J. Raynal, computer program DWBA98, NEA 1209/05 (1998).

[10] R. Machleidt, K. Hollinde, and Ch. Elster, Phys. Rep. **149**, 1 (1987).

[11] D. C. Zheng, B. R. Barrett, J. P. Vary, W. C. Haxton, and C.-L. Song, Phys. Rev. C **52**, 2488 (1995).

[12] S. Karataglidis and K. Amos, Phys. Lett. B **660**, 428 (2008), and references cited therein.

[13] B. D. Anderson, *et al.*, Phys. Rev. C **54**, 237 (1996).

[14] P. J. Dortmans, K. Amos, and S. Karataglidis, Phys. Rev. C **55**, 2723 (1997).